Morphology and Luminecent property of ZnO: Zn nanorod films prepared by thermal vapor deposition method

Weiwei Zhang, Junying Zhang, Yi Yu, Liang Cong, Ziyu Chen, Tianmin Wang
School of Science, Beihang University, Beijing 100083, China
TEL: +86-10-82315351, E-mail: zjy@buaa.edu.cn
Keywords: ZnO: Zn, photoluminescence, morphology, photocatalytic activity

Abstract

ZnO: Zn films have been deposited on the glass substrates using thermal vapor deposition method. Different morphologies such as ZnO slice, pillar and nanorod have been derived. The relationship between photoluminescence and morphology has been studied. Photocatalytic activity has been performed to validate that defects play an important role in the photoluminescence process.

1. Introduction

The ZnO as a traditional semiconductor has been studied for over a century [1]. Because of its attractive properties of non-toxicity, good electrical, optical and piezoelectric behavior, stability in a hydrogen plasma atmosphere and low price [2], the interest of research in ZnO has been regained and impressive progress has been acquired since the past few years. ZnO semiconductor has direct wide band gap (Eg~3.3eV at 300K) [3] and can be easily doped with impurity such as Al [4], Li [5] and Cu [6]. Due to the plenty of oxygen vacancies and other defects, pure ZnO can exhibit abundant color emission ranging from ultraviolet to green, which will have a great prospect in the application of vacuum fluorescent display (VFD), field emission display (FED) and other optical or optoelectronic devices as well. After annealing in the Zn vapor or reducing atmosphere, the green emission intensity was greatly improved attributing to the Zn excess. But relation between luminescence and morphology of the ZnO was rarely studied. Therefore in this paper green-emitting ZnO: Zn films were prepared via thermal vapor deposition method and the morphology of green-emitting ZnO: Zn films was studied. The relationship between photoluminescence property and morphology has been studied. Photocatalytic activity has been performed to validate that defects play an important role in the photoluminescence process.

2. Experimental

The ZnO nano particulate thin films were prepared by dip-coating process. In a typical process, equal molar $Zn(CH_3COO)_2 \cdot 2H_2O$ and ethanolamine were dissolved by ethanol in a distillation apparatus, and then boiled at 75 ^oC until a transparent sol was obtained. ZnO nano particulate films were deposited on the glass substrate by dip-coating the ZnO sol and then annealed at 450 ◦C in the air for 10min to eliminate organic group. Then the as-obtained ZnO thin films and ZnO powder for vaporing were placed in the thermal vapor deposition system, as shown in Fig. 1. First pure nitrogen was introduced into the quartz tube as purging gas to exclude the oxygen for a while. Then the furnace was powered on, with the re-firing temperature of 750 ^oC and the holding time of 30 min. Meanwhile, the mixture of nitrogen and hydrogen were introduced into the system with the flow rate fixing at 50 L/min and 40 mL/min, respectively. Finally, the samples were slowly cooled down in the furnace, and the mixture of nitrogen and hydrogen was switched off once the temperature of the furnace was lower than 100 ^oC.

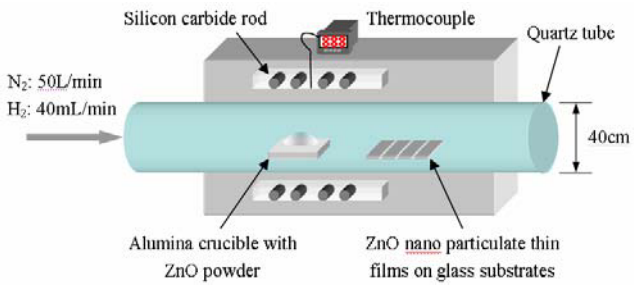

Fig. 1. Schematic illustration of the high temperature thermal vapor deposition system.

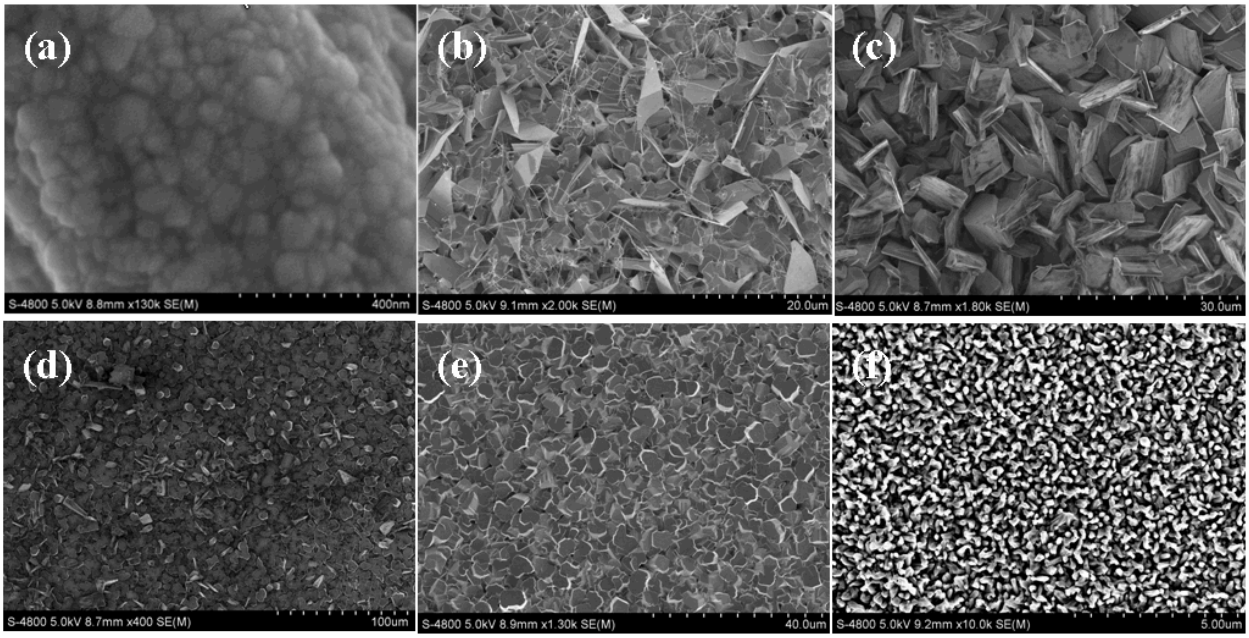

Fig. 2. SEM micrographs of ZnO films with different morphologies: (a) ZnO particulate, (b) ZnO slice, (c) ZnO blade, (d) mixture of ZnO blade and pillar, (e) ZnO pillar and (f) ZnO nanorod.

The morphology of the film was examined by S-4800 scanning electronic microscope (SEM). The X-ray Diffraction pattern was obtained by Rigaku D/MAX-2200 X-Ray Diffractometer. The excitation and emission spectra of the samples were recorded with Hitachi F-4500 fluorescence spectrometer.

3. Results and discussion

The SEM micrograph in Fig. 2 shows morphologies of ZnO: Zn films at different distances from the vapor source. Since the heating units were fixed surrounding the area of ZnO powder rather than the whole quartz tube, there existed an obvious temperature gradient. Thus the temperature of the thermocouple was the one at the ZnO vapor source and the temperature decreased as the position increased from the vapor source because of radiation loss. The ZnO thin film nearest-neighboring the end of quartz tube experienced the lowest temperature, and the surface morphology remained particulate. As approaching the ZnO vapor source, i.e. as increasing the substrate temperature, on the ZnO particulate thin film grew up sequentially the ZnO whisker, ZnO blade, ZnO pillar, and ZnO nanorod. The mechanism of the different morphologies can be attributed to the VLS growth mechanism [7-8] considering our vapor deposition system. In our study, two aspects of the growth process should be taken into consideration, which were the general growth kinetics of the different structures and the mechanism of the different morphologies. In general, the process involved the reduction of ZnO powder by hydrogen to form Zn and H_2O vapor in the high-temperature zone of 750 ^oC. The Zn vapor was transported to the substrates located downstream at a lower temperature to form Zn droplet. As the Zn droplet became supersaturated, crystalline ZnO were formed, possibly due to the reaction between Zn and H_2O or residual oxygen. The morphology difference resulted from the temperature and Zn vapor density variance. For the substrate of lowest temperature (nearest neighboring the end of quartz tube), there were insufficient nucleation kinetics or Zn source for deposition, attributed to the low temperature and rare Zn vapor density. Thus the surface morphology did not experience any change, remaining particulate (Fig. 2a). As approaching the center of the quartz tube, the density of the Zn vapor and substrate temperature increased. And there grew up the ZnO slice (shown in Fig. 2b). As the distance between the substrates and the ZnO source decreased, the temperature of the substrates increased and the surface morphologies transferred from the ZnO blade (Fig. 2c) to ZnO pillar (Fig. 2d). That is because the high density of Zn vapor offered the reagent more sufficiently and the high temperature guaranteed the crystallization. The ZnO nanorods were formed on the substrate nearest to the ZnO vapor source. It is suggested that the approximation of the temperature difference between the substrate and the vapor source induce a great amount of Zn droplet. Then the nucleus

remained in nano scale and acted as seed crystal in the high temperature. Therefore, in the reductive atmosphere ZnO preferred to grow along the (001) direction and a great amount of ZnO nanorods (Fig. 2e) were rapidly formed. Due to the consumption of Zn vapor ZnO pillar (Fig. 2d) was formed. Our results suggested that the morphologies of ZnO exhibit temperature dependence.

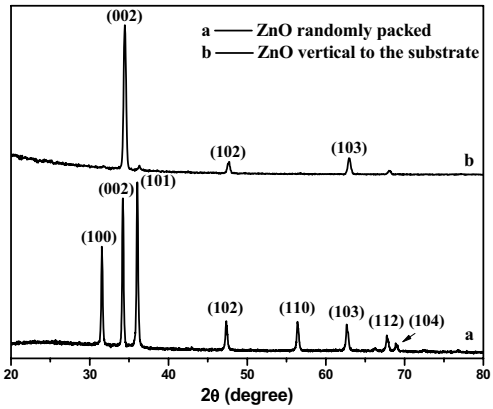

Fig. 3. XRD patterns of as-derived ZnO films on the glass substrate: a. ZnO randomly packed on the glass substrate, b. ZnO with preferential growth along (001) direction on the substrate (vertical to the substrate)

Fig. 3 shows the XRD patterns of ZnO with different morphologies. Fig. 3a shows the typical wurtzite structure corresponding to the slice, blade, pillar or nanorods randomly packed on the glass substrate, while Fig. 3b indicates excellent (001) orientation on a large area which were vertical to the substrates.

Under UV light irradiation, as-deposited ZnO films with different morphologies exhibited green emission. The room temperature photoluminescence of the ZnO films was evidenced and shown in Fig. 4. A broad intensive emission peaked at 515 nm was observed excited by UV light of 373 nm. Fig. 5 illustrates the room-temperature PL spectra of ZnO nanorods, pillar and blade formed at high, medium, and low temperature zones, respectively. The emission spectrum of Fig. 5a can be Gaussian fitted to three bands with peaks at about 483 nm, 515 nm and 544 nm as shown in the insert of Fig. 5, which means that there exist three emission centers for the ZnO nanorods. Moe Børseth et al. [9] have annealed single crystalline ZnO in inert, Zn-rich and O-rich atmospheres, and found that annealing in O_2 results in a PL at 2.35 eV (528 nm), whereas annealing in the presence of metallic Zn results in PL at 2.53 eV (490 nm). The authors attribute the former band to zinc vacancy (V_{Zn})-related defects and the latter to oxygen vacancy (V_O)-related defects, which is supported by the further study [10]. Thus the emissions at 483 nm and 515 nm are perhaps associated with the oxygen vacancy and zinc vacancy, respectively, which can easily form in the reductive atmosphere. Some reports ascribe the emission at 550nm to Li-related defects [9], while in our experiments there is no source for the doping of Li ion, and hence the yellow emission band is perhaps associated with other defects. Moreover, the ZnO nanorods films exhibited the strongest green emission due to the larger surface-to-volume ratio comparing with ZnO pillar and blade (Fig. 5a and 5b), resulting in the high concentration of defects.

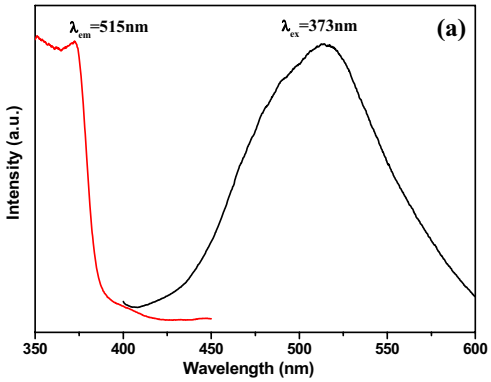

Fig. 4. Room temperature PL excitation (PLE) spectrum of ZnO: Zn nanorod film monitored at 515 nm and PL spectrum excited at 373 nm

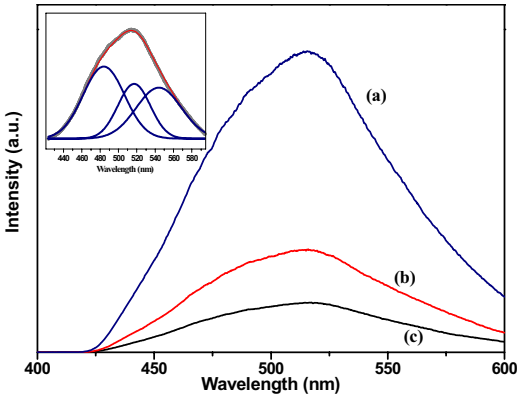

Fig. 5. PL spectra of ZnO films with different morphologies: (a) ZnO nanorod, (b) ZnO pillar and (c) ZnO slice. Inserted is the gauss-fitted spectrum of (a).

To further validate the green emission mechanism, the ZnO nanorods films were annealed in air for 10 hours at 500 °C and the PL performances and

photocatalytic activities were measured as shown in Fig. 6. Moreover, the defects like V_O can capture photo-generated electrons and reduce the recombination of the electrons and holes which is good for photocatalitic activity. However, the annealing process can fill the oxygen vacancies with oxygen and reduce the amount of V_O. Therefore, the as-deposited ZnO nanorods films exhibited higher photocatalitic activity than the one annealed in air, of which the concentration of V_O was reduced. Meanwhile the annealed ZnO nanorods films exhibited weaker green emission which was attributed to the decreasing of defects like V_O [11] as shown in Fig. 6.

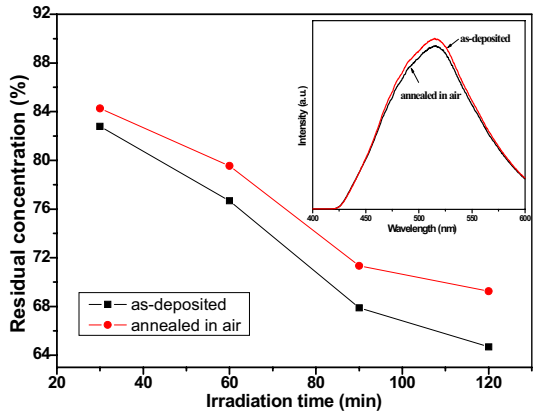

Fig. 6. Photocatalytic activities of as-deposited ZnO nanorods and that annealed in air for 10 hours. Inserted is the PL spectra of the ZnO nanorods mentioned-above excited by 373 nm.

4. Summary

In the summary, ZnO films with different morphologies were derived on the ZnO particulate films simply by thermal vapor process in the reductive atmosphere. The morphologies show intensive temperature dependence and ZnO slice, pillars and nanorods were formed at high, medium, and low temperature zones, respectively. Under the irradiation of 373 nm UV light, ZnO films with all morphologies exhibited green emission, of which the one with nanorods showed the strongest intensity. Moreover, further study between as-deposited ZnO nanorods film and that annealing in air showed that the former stronger PL intensity, and higher photocataly acitivity attributed to the V_O which supported the important role V_O played in the PL process.

5. Acknowledgements

This work was supported by Program for New Century Excellent Talents in University under Grant No. NCET-06-0179 and National Natural Science Foundation of China under Grant No. 50672003.

6. References

1. A. van Dijken, E. A. Meulenkamp, D. Vanmaekelbergh, A. Meijerink, *J of Lumin*, **87-89[454-456]**, (2000).
2. R.G. Gordon, MRS Bull. **25[52]**, (2000).
3. Ü. Özgür, Ya. I. Alivov, C. Liu, A. Teke, M. A. Reshchikov, S. Doğan, V. Avrutin, S.-J. Cho, and H. Morkoç, *J of Appl. Phys*, **98[041301-103],** (2005).
4. H. Kim, C. M. Gilmore, J. S. Horwitz, A. Pique´, H. Murata, G. P. Kushto, R. Schlaf, Z. H. Kafafi, and D. B. Chrisey, *Appl. Phys. Lett*, **76[259-261]**, (2000).
5. D. Zwingel, *J of Lumin*, **5[385-405]**, (1972).
6. F. Leiter, H. Zhou, F. Henecker, A. Hofstaetter, D.M. Hofmann, B.K. Meyer, Physica B, **308-310[908-911]**, (2001)
7. R. S. Wagner, W. C. Ellis, *Appl. Phys. Lett*, **4[89]**, (1964).
8. B. D. Yao, Y. F. Chan, and N. Wang, *Appl. Phys. Lett*, **81[757-759]**, (2002).
9. T. Moe Børseth, B. G. Svensson, A. Yu. Kuznetsov, P. Klason, Q. X. Zhao, M. Willander, *Appl. Phys. Lett*, **89[262112]**, (2006).
10. Peter Klason, Thomas Moe Børseth, Qing X. Zhao, Bengt G. Svensson, Andrej Yu. Kuznetsov, Peder J. Bergman, Magnus Willander, *Solid State Communications*, **145[321-326]**, (2008).
11. L. Q. Jing, Y. C. Qu, B. Q. Wang, S. D. Li, B. J. Jiang, L. B. Yang, W. Fu, H. G. Fu, J. Z. Sun, *Solar Energy Materials & Solar Cells*, **90[1773-1787]**, (2006).